pollutants

MDPI

Article

Environmental Profile Assessment in a Highly Industrialized Area Through Magnetic Susceptibility Spatial Variations and Morphological Study of Magnetic Particles: The Case of Sarigiol Basin (Greece)

Chrysoula Chrysakopoulou *, Elina Aidona, Dimitrios Vogiatzis, Alexandros Drakoulis, Lambrini Papadopoulou and Nikolaos Kantiranis

School of Geology, Faculty of Sciences, Aristotle University of Thessaloniki, 54 124 Thessaloniki, Greece; aidona@geo.auth.gr (E.A.); dvogias@geo.auth.gr (D.V.); alexdr@geo.auth.gr (A.D.); lambrini@geo.auth.gr (L.P.); kantira@geo.auth.gr (N.K.)

* Correspondence: chrysako@geo.auth.gr

Abstract: Two sets of sediment samples were collected from the Sarigiol basin, Greece, aiming to evaluate the environmental consequences of the industrial activity in the area by assessing their magnetic properties with the magnetic susceptibility method. Chemical composition and morphological characteristics of magnetic particles were defined by EDX analysis and scanning electron microscopy, respectively. Based on the results, most of the study area shows positive values of the difference between X_{LF} values of the samples, indicating the influence of fly ash dispersion from Agios Dimitrios and Kardia power plants and the conveyor belt, down to a depth of 50 cm. Negative values in the NE, W and S parts of the study area are attributed to ophiolite complexes. Anthropogenic and lithogenic magnetic particles were identified at a 50 cm depth, in the form of spheres and octahedrons, respectively. Fe is the dominant element while Al, Si, Mg and Ca were found in minor amounts. Cr increases with depth, pointing mainly to a lithogenic source, while Ti decreases, suggesting a relationship with the dispersed fly ash particles. Mn and Zn were found in limited magnetic spheres. These findings highlight the need for effective environmental management strategies and are valuable keys for soil pollution control.

Keywords: magnetic susceptibility; pollution; sediments; soil; Sarigiol basin; Greece

check for updates

Academic Editor: Raimundo Jimenez-Ballesta

Received: 15 November 2024
Revised: 5 February 2025
Accepted: 12 February 2025
Published: 17 February 2025

Citation: Chrysakopoulou, C.; Aidona, E.; Vogiatzis, D.; Drakoulis, A.; Papadopoulou, L.; Kantiranis, N. Environmental Profile Assessment in a Highly Industrialized Area Through Magnetic Susceptibility Spatial Variations and Morphological Study of Magnetic Particles: The Case of Sarigiol Basin (Greece). *Pollutants* **2025**, *5*, 4. https://doi.org/10.3390/pollutants5010004

Copyright: © 2025 by the authors. Licensee MDPI, Basel, Switzerland. This article is an open access article distributed under the terms and conditions of the Creative Commons Attribution (CC BY) license (https://creativecommons.org/licenses/by/4.0/).

1. Introduction

In the past century, continuous urbanization and industrialization have led to an environmental scourge which has become dramatically evident in recent decades. The entire scientific community is trying with all the means at its disposal to assess this damage and determine the ways in which it can be limited. Environmental pollution is not a phenomenon of recent years, however, over the years its presence has become more and more intense, being one of the most important problems that the human species has to face. In 2015, diseases from environmental pollution were predicted to result in the premature death of 9,000,000 people [1] while Adami et al. [2] argued that long-term exposure to PM_{10} particulate matter concentrations of more than 30 $\mu g/m^3$ results in an increased risk of developing autoimmune diseases.

Soil is one of the largest sinks for environmental pollutants. Coal burning, vehicular traffic, steel iron manufacturing and metal fabrication are industrial processes acting as important sources for pollutant dispersion [3]. Magnetic particles serve as excellent

indicators for environmental pollution. They mainly consist of strongly ferromagnetic minerals, such as magnetite and maghemite but also hematite and siderite. In soil, magnetic particles may derive either from the weathering and transportation of clastic material from the parent rock (mainly mafic/ultramafic rocks) or from anthropogenic activities. Iron-rich particles and their heavy metal load present in the magnetic fraction of the soil in industrial and urban areas are connected with high-temperature processes, such as coal combustion (coal-fired power plants), steel working and vehicle emissions [4]. The extensive sensitivity of the iron-bearing minerals to various environmental processes makes magnetic measurements highly effective as proxies for the monitoring of different factors influencing the environment. Over the past 20 years, magnetic susceptibility measurements have been gaining ground for the assessment of soil pollution levels in urban and industrial areas as sensitive and, at the same time, efficient, fast, non-destructive and cost-effective techniques [5–13].

Magnetic susceptibility (MS) is a parameter that allows an easy measure of the magnetic particle content, regardless of their origin [12]. Magnetite and maghemite, the main magnetic minerals for the enhancement of the magnetic susceptibility in soils, can be detected in extremely small amounts due to the most valuable advantage magnetic susceptibility has, its sensitivity. According to Dearing [14], even a small quantity of magnetite (0.01%), in typical soil magnetic populations, accounts for approximately 85% of the total magnetic susceptibility. In simple terms, susceptibility is the ratio of induced magnetization by the application of a weak magnetic field to this applied field. It is basically defined as the ability of a substance to be magnetized by an artificially applied external magnetic field [15].

High values of magnetic susceptibility do not indicate that the presence of magnetic particles is only due to anthropogenic activity but they may also indicate a lithogenic source [5]. Consequently, the question is how contamination sources can be determined and their influence can be distinguished. Some of the guidelines that have been suggested in studies throughout the years are magnetic susceptibility measurements in vertical profiles or examination of additional magnetic properties [16,17]. In Greece, plenty of studies have been performed for the determination of the magnetic signature of the soil with the magnetic susceptibility method [5,18–20]. The primary and largest lignite mining region of Greece is located in Ptolemaida–Kozani–Amyntaio basin (northern Greece). Although the post-lignite era has already begun, the footprint of the seventy years' mining activity and especially the deficient management of the produced fly ash which is dispersed all around the area is notable [21–23]. Recently, Chrysakopoulou et al. [24,25] presented the results of a study of magnetic particles in the upper soil horizons of the Sarigiol basin, indicating the environmental signature of the fly ash dispersed from the coal combustion. In Chrysakopoulou et al. [24,25], the magnetic fraction was isolated from soil and sediment samples from a depth of 10 cm. Their highest values were attributed to ophiolite complexes and fly ash dispersion from Agios Dimitrios and Kardia power plants in the E and NW parts of the area.

The magnetic susceptibility method was used for the assessment of the magnetic properties of vertical sediment profiles at Sarigiol basin in northern Greece and magnetic particles were separated from the samples in order to determine their chemical composition using energy dispersive spectroscopy analysis (EDX), while their morphological characteristics were observed via scanning electron microscopy (SEM). Magnetic susceptibility is a very sensitive tool specifically for large-scale environmental assessments and has the ability to detect the pollution level in a relatively short time range, it is also non-destructive and enables the creation of an initial map of the pollution distribution. Based on these facts, it was used as the primary technique for evaluating the environmental pollution at

Sarigiol basin. The aim of the present study is to determine the magnetic signal of these vertical sediment profiles in this highly industrialized area and to extend the results of the previous studies by searching for the presence of magnetic particles at greater depths but this time using the magnetic susceptibility method. The main purpose is to assess the impact of the anthropogenic activities in Sarigiol basin in a vertical profile and especially the effect of the dispersion and deposition of fly ash particles. The value of this study lies in the evaluation of the environmental footprint of the local coal combustion activity in the surrounding area.

2. Materials and Methods

2.1. Study Area

Sarigiol basin is located in northern Greece and belongs to the Kozani regional unit. South of the study area, there is the city of Kozani, which is the largest urban center of the region with a population of about 42,000 residents. To the north, Ptolemaida is located, the second largest city in the region after Kozani, with a population of about 32,000 [26]. The climate of the wider area of Kozani–Ptolemaida is characterized as the Mediterranean type, with an average annual rainfall of 640 mm, an average temperature of 13 °C and SSE wind direction [21]. Sarigiol basin is the southern part of the intercontinental lignite-bearing Ptolemais–Kozani–Florina basin. The perimeter of the basin is dominated by limestone formations, while ophiolite complexes, composed of many serpentine occurrences, are detected in the NE and SW parts of the area (Figure 1). There are also groups of metamorphic rocks and flysch layers. Sands, clay formations and talus/brecciated cones constitute the Quaternary formations of the central part of the research area. Sarigiol basin has been particularly studied due to the presence of lignite deposits in the wider area. It belongs to the Pelagonic geotectonic zone and the basement of the basin consists of Paleozoic and Mesozoic metamorphic and plutonic rocks [27]. The soils of the region are characterized as calcareous with alkaline pH values reflecting the presence of limestones [27].

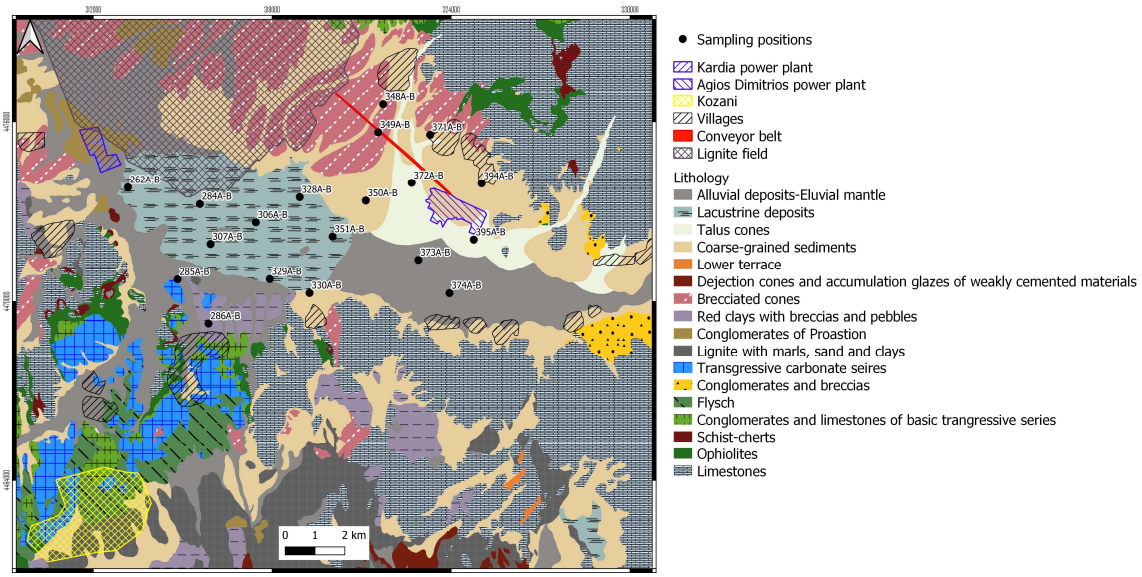

Figure 1. Lithological map of the study area (modified from EAGME) showing the prevalence of limestone rocks around the perimeter of the sampling area, the occurrences of ophiolite complexes in the NE and SW parts and the presence of sands, clay formations and talus/brecciated cones in the center of the study area.

2.2. Sampling Location and Analytical Procedures

In total, 38 sediment samples were collected from 19 different positions at depths of 0–10 cm (samples A) and 10–50 cm (samples B) (Figure 1). At first, the samples were dried at 50 °C for 4–5 days in order to remove moisture without destabilizing the magnetic particles. After that, they were grounded, placed in plastic boxes of 2 × 2 × 2 cm and weighed before the measurements started. Laboratory measurements of the mass-specific magnetic susceptibility (χ) of the samples were assessed for low (0.47 kHz) and high (4.7 kHz) frequency using a Bartingthon MS2 laboratory magnetic susceptibility meter, equipped with a dual frequency MS2B sensor at the Department of Geophysics, Aristotle University of Thessaloniki. Each sample was measured a minimum of three times, with the values averaged and adjusted to account for the temperature drift of the pick-up coil [5]. The magnetic susceptibility value serves as an indicator of the concentration of strongly ferrimagnetic minerals, such as magnetite, within the sample. Frequency dependent susceptibility (X_{FD} %) was calculated according to Dearing et al. [14] as:

$$X_{FD}\ \% = 100(X_{LF} - X_{HF})/X_{LF}$$

Minimum, maximum, median, mean and standard deviation values of the data from the magnetic susceptibility measurements were calculated with basic statistical descriptive functions of Microsoft Excel as no advanced functions were needed.

For the separation of the magnetic fraction, 20 g of representative material (<1 mm) was gently disaggregated by hand using an agate mortar. The disaggregated material was then mixed with 250 mL of deionized water and 10 mL of a dispersing agent ($(NaPO_3)_6$, 100 g/L) before being placed with a magnet in a beaker. A magnetic stirrer, operated at low speed (<100 rpm) without heating, was used in order to extract the strongly magnetic particles while ensuring proper particle dispersion. The separation process was repeated three times, with intervals of 5, 2, and 1 min, respectively [7]. Finally, for a better result, deionized water was applied with high pressure by using a nozzle to the magnetic fraction extracted from each sample in order to remove any clay material from the surface of the magnetic particles and make them more visible when observed with SEM. The final magnetic fraction extracted from each sample was dried at 110 °C until reaching a constant weight, and then it was weighed and stored in plastic vial.

The chemical composition of the magnetic fraction was determined by EDX analysis using the scanning electron microscope (JEOL JSM6390LV, Tokyo, Japan) of the Electron Microscopy Laboratory of the Aristotle University of Thessaloniki, which was employed to observe the morphology of randomly selected magnetic particles. A representative amount of the magnetic fraction of each studied sample was fixed on aluminum double-sided tapes and then placed on special sample holders. Prior to observation, they were coated with carbon. The observation was conducted by examining randomly selected optical fields. Surfer was used to map the spatial distribution of the mass-specific susceptibility values (X_{LF}) and to create the 3D model of the ΔX_{LF} which will indicate if the presence of magnetic particles in each vertical sediment profile has an anthropogenic or lithogenic source, via spatial interpolation kriging to create grids. Later, these grids were imported into QGIS 3.16.15 to create the corresponding maps. The extracted maps were presented through a scaled color gradation of filled contours based on the ranges of the magnetic susceptibility values (X_{LF}) of each sample.

3. Results and Discussion

3.1. Magnetic Properties of the Samples

The descriptive statistics of the mass-specific susceptibility (X_{LF}) and frequency dependent magnetic susceptibility (X_{FD} %) values in samples A (0–10 cm depth) and B (10–50 cm depth) are presented in Table 1. Mass-specific susceptibility (X_{LF}) values of samples A varied between 14.2 and 241.6 $\times 10^{-8}$ $m^3 \cdot kg^{-1}$ (with a median of 135.0 $\times 10^{-8}$ $m^3 \cdot kg^{-1}$), indicating enhanced levels of ferrimagnetic particles. Mass-specific susceptibility (X_{LF}) values of samples B varied between 4.1 and 223.6 $\times 10^{-8}$ $m^3 \cdot kg^{-1}$ (with a median of 133.2 $\times 10^{-8}$ $m^3 \cdot kg^{-1}$), indicating again the enhanced presence of ferromagnetic particles at the depth of 10–50 cm, and they are slightly lower than those of samples A but still similar. The frequency dependent magnetic susceptibility (X_{FD} %) for samples A exhibited a wide range of 0–9.5% (median 5.0%) while the corresponding values for samples B varied between 0 and 9.17% (median 4.65%).

Table 1. Descriptive statistics of magnetic properties of the studied samples A (depth 0–10 cm) and B (depth 10–50 cm) in Sarigiol basin.

		A					B				
Variable	**Unit**	**Median**	**Mean**	**SD** [1]	**Min**	**Max**	**Median**	**Mean**	**SD** [1]	**Min**	**Max**
X_{LF}	$\times 10^{-8}$ $m^3 \cdot kg^{-1}$	135	114.5	82.2	14.2	241.6	133.2	104.9	80.6	4.1	223.6
X_{FD}	%	5.0	4.82	2.81	0	9.50	4.65	4.64	2.77	0	9.17

[1] Standard deviation.

Numerous factors influence the magnetic susceptibility of the soils, including the parent materials of the background, as well as the developmental direction and extent of iron-bearing minerals they contain [28]. Magnetic minerals occur as iron oxides (e.g., magnetite, maghemite, hematite), oxyhydroxides (e.g., goethite, ferrihydrite, lepidocrocite) and sulfides (e.g., pyrrhotite) [29]. The total ferromagnetic content in soil may include primary minerals such as titanomagnetite with lithogenic origin, secondary minerals such as magnetite and maghemite with bacterial and chemical origin or formed during burning and magnetic spherules originating from anthropogenic pollution [14]. Fly ash particles, the main pollutants of the soils, steel manufacturing, vehicle emissions and agricultural activities are significant sources for the presence of magnetic particles of anthropogenic origin.

Figure 2a,b show the spatial distribution of the mass-magnetic susceptibility (X_{LF}) for samples A at the depth of 0–10 cm and samples B at the depth of 10–50 cm, respectively.

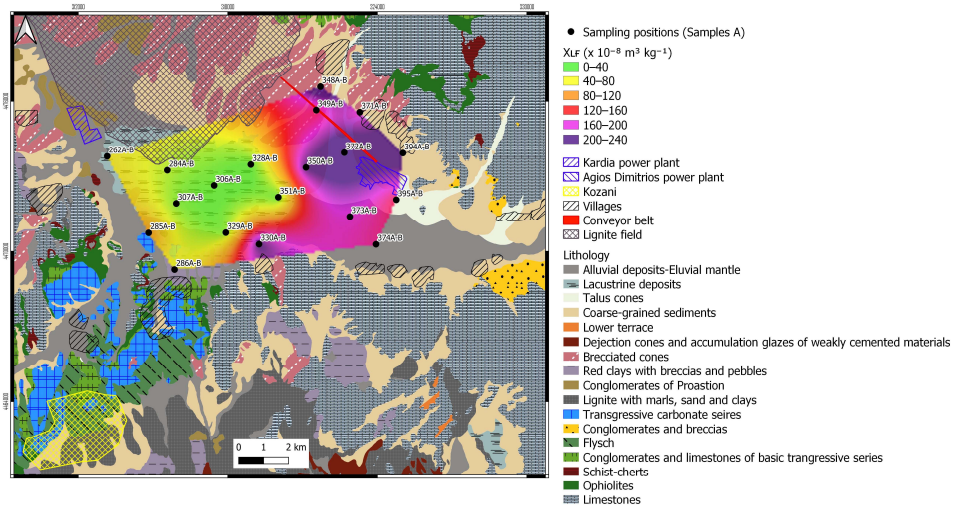

(**a**)

Figure 2. *Cont.*

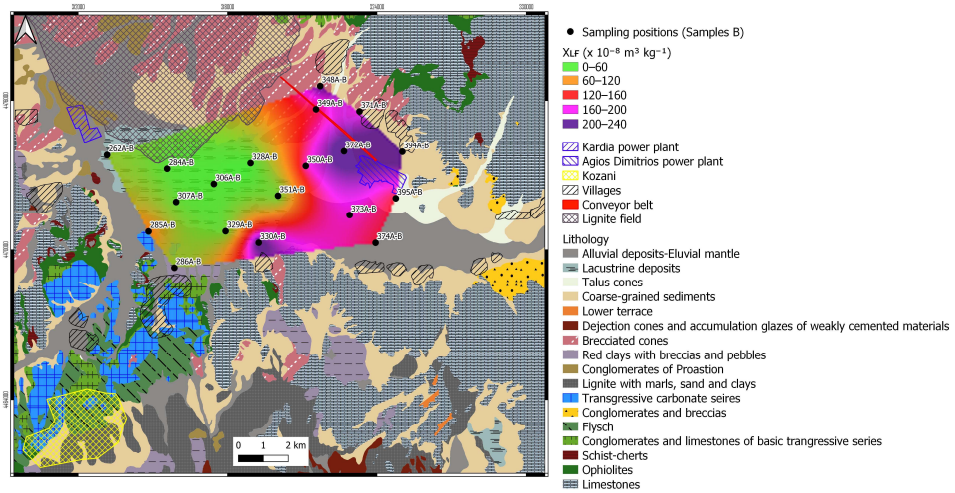

(**b**)

Figure 2. Spatial distribution of the magnetic susceptibility values in the study area for (**a**) samples A at the depth of 0–10 cm; (**b**) samples B at the depth of 10–50 cm. Highest values of the magnetic susceptibility for both samples A and B are shown in purple in the NNE, E and S parts of Sarigiol basin while the lowest value are depicted in bright green in the center of the area.

The highest values of the studied samples A are shown in the NNE, E and S parts of the study area (>200 $\times$ 10^{-8} $m^3 \cdot kg^{-1}$) while the lowest are found in the center part of the area. The high values in the NNE and E parts are located near the Agios Dimitrios power plant and the conveyor belt but also SW of an ophiolite complex. In the S part, there are also some ophiolite rocks but not to the same extent. In our previous work [24], the results from the separation of the magnetic fraction for samples at a depth of 0–10 cm showed almost the same spatial distribution, with the highest values of the magnetic fraction appearing in the NNE part and locally in the S and NW parts, while the average value was below 1 wt.%. Figure 2b displays the spatial distribution for the deeper samples B (10–50 cm) with the highest values having the exact same distribution as samples A (NNE, E and S parts of the study area) but, at this depth, the lowest values in the center tend to extend to the N part of the study area.

High values of magnetic susceptibility of samples show an increased amount of ferrimagnetic minerals. Aidona et al. [5] studied vertical soil profiles (depth of the samples was 0–10 cm and 60–70 cm) near Anthemountas River in Thessaloniki (northern Greece) and they found values of X_{LF} between 50 and 450 $\times$ 10^{-8} $m^3 \cdot kg^{-1}$, indicating both the anthropogenic and lithogenic influence at the samples. In samples of a 10 cm depth from the broader area of Megalopolis power plant (Peloponnese), X_{LF} values ranged between 4.3 and 613.8 $\times$ 10^{-8} $m^3 \cdot kg^{-1}$ [18], showing the impact of the dispersion and deposition of the fly ash. In addition, topsoil samples (0–10 cm) from Krakow (southern Poland) have been studied in order to detect their magnetic signal as a steelwork industrial plant and coal-fired power plant are located in the broader area. X_{LF} values ranged between 11.8 and 434.6 $\times$ 10^{-8} $m^3 \cdot kg^{-1}$ [30]. Topsoil samples from a commercial area, a motor park and a school environment in northeast Nigeria were studied using magnetic proxy parameters in order to detect pollution hotspots [31]. The results of the mass-specific low frequency magnetic susceptibility measurements showed significant enhancement (mean values 191.61, 901.34 and 574.92 $\times$ 10^{-8} $m^3 \cdot kg^{-1}$). Soil type is an important factor, controlling the enrichment of ferromagnetic particles in soil profiles. However, topsoil (0–20 cm) samples from Austrian provinces Lower Austria and Burgenland showed a magnetic enrichment relative to subsoil (40–50 cm) samples depending more on the underlying parent material than on the soil type [32].

The difference between the topsoil and subsoil magnetic susceptibility values is the most common approach for the detection of anthropogenic anomalies. In Figure 3, a 3D model depicts the difference of the low-field mass-specific magnetic susceptibility (ΔX_{LF}) values between samples A (0–10 cm) and samples B (10–50 cm) in the study area. Hybomas (positive values) indicate anthropogenic anomalies, in contrast to pits (negative values) where the magnetic particles have mainly lithogenic origin. In Figure 4, a map of the spatial distribution of these differences is presented with color ranges.

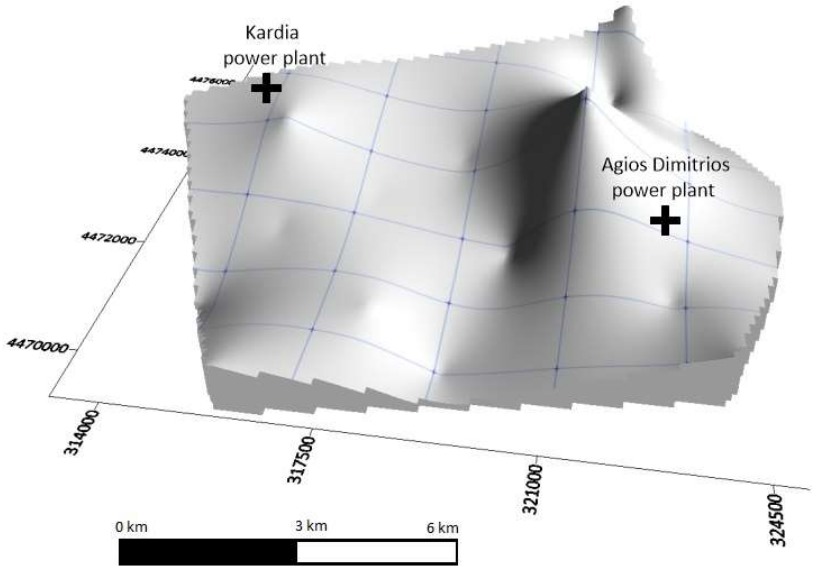

Figure 3. Spatial distribution of the difference of the low-field mass-specific magnetic susceptibility (ΔX_{LF}) values in the study area with a 3D model with hybomas for positive values and pits for negative values. Highest hyboma (indicating anthropogenic influence) is shown W of Agios Dimitrios power plant while pits (lithogenic influence) are particularly evident in the S part of the study area.

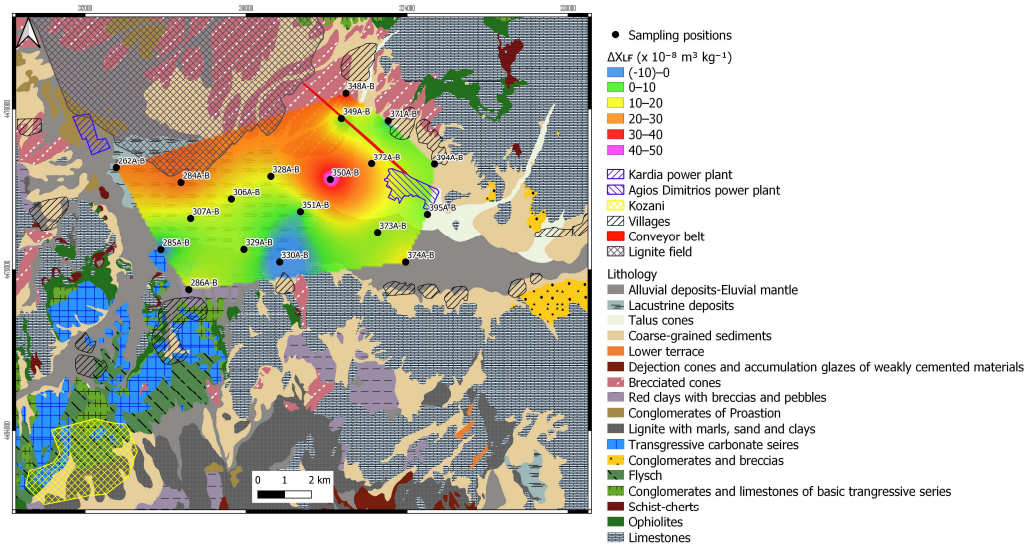

Figure 4. Spatial distribution of the difference of the low-field mass-specific magnetic susceptibility (ΔX_{LF}) values in the study area for the total of the samples, where the highest value is shown in pink W of Agios Dimitrios power plant (E part of study area) and lower values are depicted in blue in the S and W parts of the study area.

Based on Figure 3, negative values are shown in the S part of the study area and locally in the NE and W parts. The scattered occurrence of ophiolite complexes in the S and W parts of the basin seems to play a primary role in the magnetic properties of this part of the study

area as weathered ultramafic fragments of these complexes are transported and deposited along the SW perimeter of the Sarigiol basin. The extensive appearance of ultramafic rocks in the NE part of the basin is probably the source of the pit in this part. As shown in the 3D model (Figure 3) and the spatial distribution map (Figure 4), most of the study area shows positive values of ΔX_{LF} (hybomas), indicating the influence of anthropogenic activities and especially of the fly ash dispersion and deposition up to half a meter below the ground surface. The highest positive values of ΔX_{LF} are presented northwest of Agios Dimitrios power plant (E part of the study area) and north of the conveyor belt (NE part of the study area).

Magnetic susceptibility in vertical profiles has also been studied by other researchers, leading to the similar findings. Hanesch and Scholger [32] reported high values of magnetic susceptibility in the uppermost 20 cm of the soil, indicating an anthropogenic influence, whereas lower values reflect the dominance of lithological influence. If this difference exceeds 20×10^{-8} $m^3 \cdot kg^{-1}$, then an anthropogenic anomaly is identified. On the contrary, if the difference is below -20×10^{-8} $m^3 \cdot kg^{-1}$, the anomaly is controlled by lithology. In the present study, ΔX_{LF} values $> 20 \times 10^{-8}$ $m^3 \cdot kg^{-1}$ are found in the N part of the area, along the entire S side of the South Field with a maintenance tendency to the E part (west of the Agios Dimitrios power plant and the conveyor belt). However, it does not mean that, in the remaining part of the study area where the positive values of the ΔX_{LF} are less than 20×10^{-8} $m^3 \cdot kg^{-1}$, anthropogenic pollution has no influence, as the area is strongly industrialized in combination with agricultural activities. Also, the prevailing wind direction in the Ptolemais–Kozani–Amyntaio basin is NNW [25], a factor that significantly participates in the dispersion of fly ash in the area, enhancing the results of the magnetic susceptibility measurements. Sarris et al. [18] identified wind as a key factor controlling the values of magnetic susceptibility, with high X_{LF} values of topsoil samples (0–10 cm depth) from the broader area of Megalopolis power plant (Peloponnese) being orientated parallel to the wind direction. The same assumption of $\Delta X_{LF} > -20 \times 10^{-8}$ $m^3 \cdot kg^{-1}$ applies to the studied samples that showed negative ΔX_{LF} values of $< -20 \times 10^{-8}$ $m^3 \cdot kg^{-1}$, as their positions were directly affected by ophiolite rock complexes. According to researchers, soils that have been affected by anthropogenic pollution showed decreased values of magnetic susceptibility with depth [33–35]. Magiera et al. [16] sought to differentiate the lithogenic and anthropogenic influence on topsoil by measuring magnetic susceptibility. Their study of the vertical profiles revealed higher values in the forest topsoils and lower values in subsoils of polluted areas.

Frequency dependent magnetic susceptibility (X_{FD} %) corresponds to the presence of ultrafine or superparamagnetic (SP) ferrimagnetic grains in a material. This parameter is sensitive only to a very narrow grain size region (approximately 0.018–0.020 μm in diameter) crossing the superparamagnetic/single-domain threshold [31]. Ferrimagnetic particles which belong to this grain domain tend to have lithogenic origin [36]. Coarser mutlidomain (MD) magnetic grains are more frequent in wastes of industrial processes (e.g., fly ash) or in vehicle emissions and brake dust [31]. Figure 5a,b show the spatial distribution of the X_{FD} % values for both sets of samples.

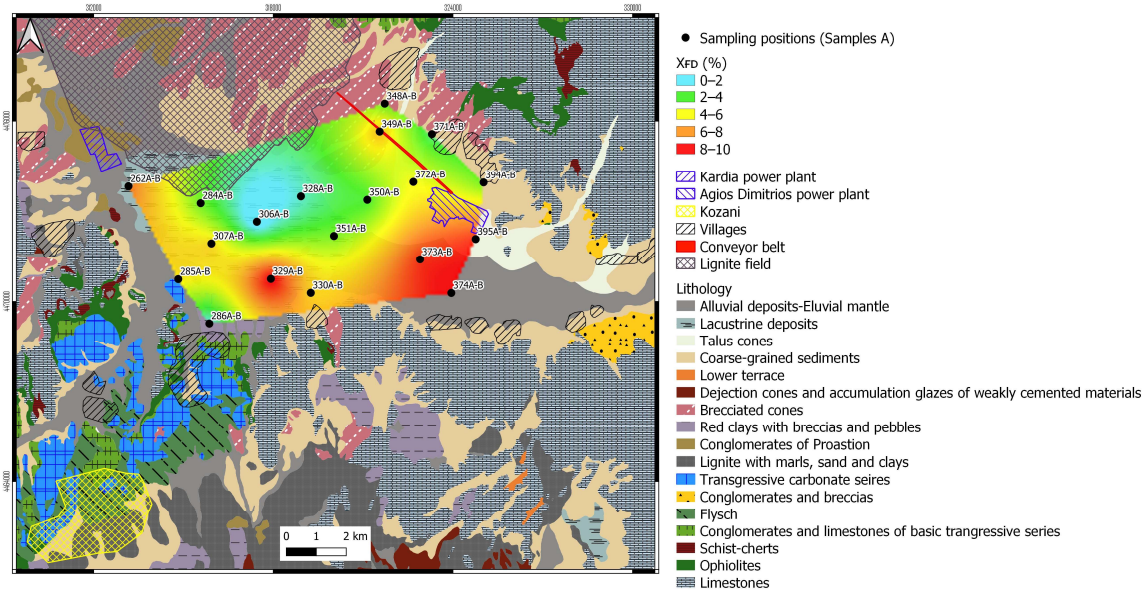

(**a**)

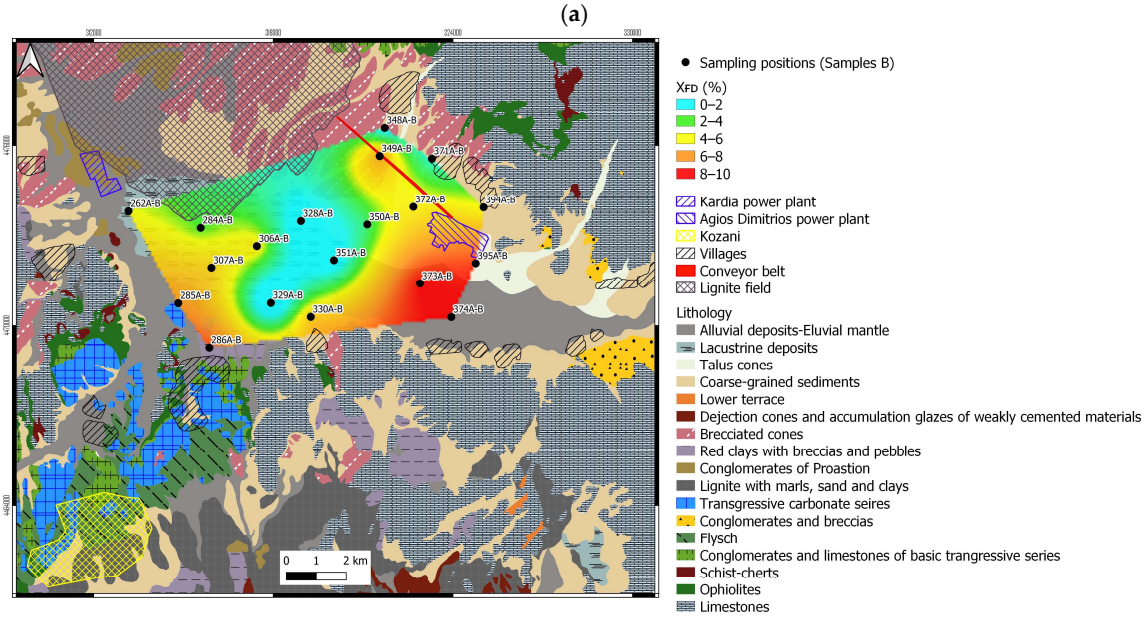

(**b**)

Figure 5. Spatial distribution of the frequency-dependent magnetic susceptibility (X_{FD} %) values in the study area for (**a**) samples A at the depth of 0–10 cm; (**b**) samples B at the depth of 10–50 cm. Highest values for the total of the samples are depicted in red in the SE and locally in the S and W parts of Sarigiol basin. Lowest values for both samples A and B are shown mainly in the central part of the study area in light blue.

The highest values (approx. 9%) for the sets of samples are spatially limited to the SE part of the area and locally to the S and W parts of the basin for samples A and B, respectively. Based on these results, in these parts of the study area SP grains probably from pedogenic processes seem to be present in significant amounts. The X_{FD} % values of the studied samples are presented with corresponding low-field mass-specific magnetic susceptibility (Figure 6).

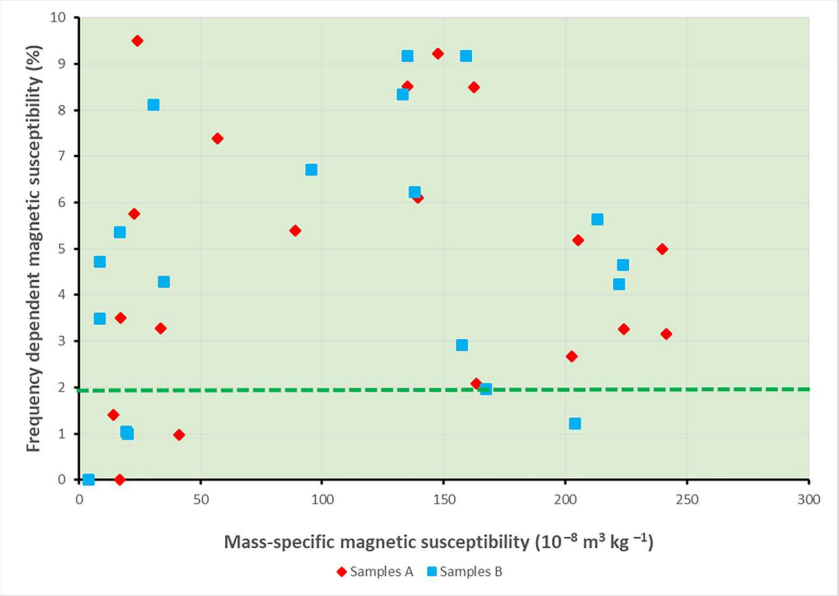

Figure 6. Plot of low-field mass-specific magnetic susceptibility versus frequency dependent magnetic susceptibility of the studied samples of Sarigiol basin. The majority for both sets of samples shows X_{FD} % values between 2 and 10% indicating the admixture of SP and coarser non-SP grains or SP grains even smaller than 0.018 μm based on Dearing's model (Table 2) while the correlation with X_{LF} values seems very weak.

Many authors have tried to correlate the X_{FD} % with X_{LF} in order to find out whether there is just a lithogenic influence or an anthropogenic anomaly in an area. According to Dearing's model [36], an X_{FD} % of 5% or more indicates that the superparamagnetic (SP) particles are present in significant amounts while for values < 5% magnetic properties are controlled by coarser-grained magnetic particles with anthropogenic source. In another study of his [14], he proposes a model for the interpretation of frequency dependence as follows:

Table 2. Dearing's model [14] for the interpretation of frequency dependence (X_{FD} %).

X_{FD}%	Value	Interpretation
Low	<2.0%	Virtually no SP grains
Medium	2–10%	Admixture of SP and coarser non-SP grains or SP grains (<0.005 μm)
High	10–14%	Virtually all (>75%) SP grains
Very high	>14%	Rare values, erroneous measurements, weak samples or contamination

Superparamagnetic grains may originate from the weathering of the parent rocks or the fragmentation of larger ferromagnetic grains. Findings from a set of samples along the estuary of the Krueng Aceh River in the city of Banda Aceh, Indonesia, demonstrate that X_{LF} and X_{FD} values offer a distinction that can be used to identify the pollution source [37]. Han et al. [38] established the threshold of X_{FD} < 3%, with values exceeding this indicating the presence of certain amount of SP particles and a specific level of soil development, which is strongly influenced by natural conditions (i.e., parent materials). Polluted soils near a highway in Beijing City, Quaternary loess and unpolluted soils derived from volcanic rocks were studied in order to measure their magnetic susceptibility [28]. The authors conclude that, the higher the X_{LF}, the lower the X_{FD} and the more seriously the soil may be polluted and they also set the limit of X_{FD} < 3% for the polluted samples. They further indicate that samples with X_{LF} value > 100 × 10^{-8} $m^3 \cdot kg^{-1}$ and an X_{FD} value < 3% are possibly polluted.

Figure 6 shows that 9 out of 19 samples A and 9 out of 19 samples B have an X_{FD} value greater than 5%, implying that the contribution of SP particles, due to pedogenic processes, is considerable [14,36]. The correlation between X_{LF} and X_{FD} values is very poor, in combination with the fact that accepting Dearing's limit of 5%, seven out of nineteen sample positions (329, 349, 351, 371, 373, 374, 395) do not follow this admission based on the values of ΔX_{LF}. Furthermore, none of the samples fits the assumption that with the increase in X_{LF} the decrease in X_{FD} % indicates an anthropogenic anomaly (Figure 6). The latest Dearing's model (Table 2) seems to be able to best interpret the X_{FD} % values for the studied samples. The majority of the samples have medium X_{FD} % values between 2 and 10%, indicating an admixture of SP and coarser non-SP grains or SP grains even smaller than 0.018 μm. This practically means that, for the majority of the samples, the contribution of the fly ash particles cannot be excluded as the wider Ptolemaida–Kozani area is heavily industrialized. For samples 351A-B and 371A-B with X_{FD}% < 2% which correspond to coarser multidomain (MD) grains, the contribution of magnetic particles with an anthropogenic source must be taken into account, even if they have a negative ΔX_{LF} value (Figure 3), indicating the lithogenic origin of the magnetic particles.

3.2. Morphological Characteristics and Elemental Analysis

The magnetic fraction from a subset of the studied samples with X_{LF} value > 100 $\times 10^{-8}$ $m^3 \cdot kg^{-1}$ was examined using SEM, as the morphological characteristics as well as their elemental composition provide a path for their correlation with anthropogenic sources [39]. Our previous work has shown that anthropogenic magnetic particles (AMPs) in the form of spheres were found at a depth of 0–10 cm, with simple or more complex surface structures [25]. In this study, magnetic spheres were also identified in samples B at the depth of 10–50 cm (Figure 7a–f). This specific morphology of the magnetic particles is associated with the high-temperature combustion of fossil fuels and is primarily a component of the fly ash produced during this process. The presence of these magnetic spheres is attributed to the fly ash produced by the activity of the two electric power plants in the study area, Agios Dimitrios and Kardia, located in the E and NW parts of the basin, respectively, without excluding the contribution of particles from the exhausts of vehicles and agricultural machinery.

The size of the magnetic spheres ranges between 11.3 and 90 μm while the majority of them are 10–50 μm, as well as the majority of the identified magnetic spheres in samples A (depth of 0–10 cm). Their surface is either smooth (Figure 7a) or more often complex, with different surface patterns such as spongy (Figure 7b), thread (Figure 7c) and blocky type (Figure 7d), some of them having a more harsh surface or aluminosilicate aggregates (Figure 7e,f). The aggregation or the loss of sphericity in these particles is likely the result of heterogeneous condensations occurring during their transportations [40]. All these types of structures are very often present in all fly ash particles during coal combustion. There is a multifactorial model controlling their size distribution and, further, the transportation path. Coal type and parameters (granulation, chemical composition, mode of occurrence of chemical compounds), combustion process parameters (temperature, oxygen concentration) and boiler are the major factors controlling the particle size. The applied air pollution control devices (electrostatic precipitators, fabric filters and flue gas desulfurization installations), meteorological conditions, height of the chimneys and the distance of the power plants dictate the transportation and finally the deposition path [40].

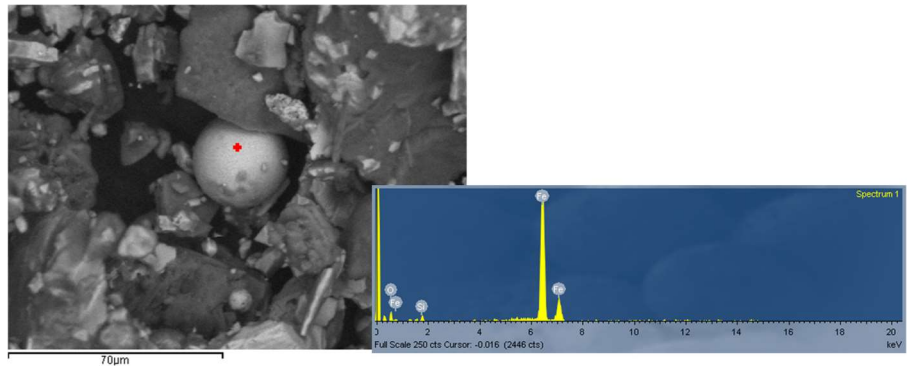

(**a**)

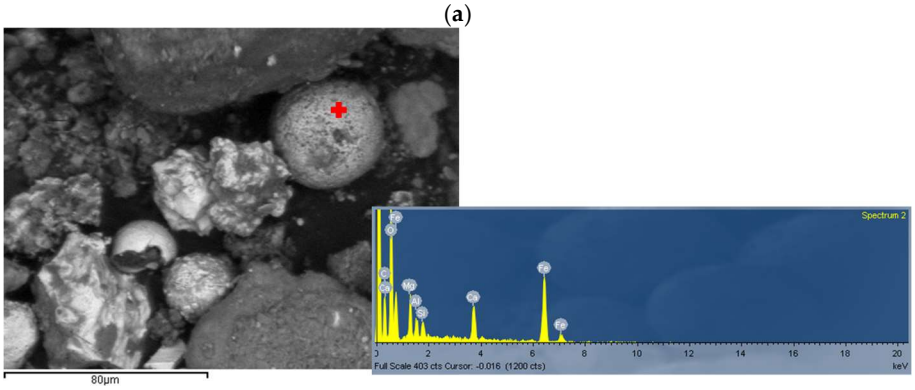

(**b**)

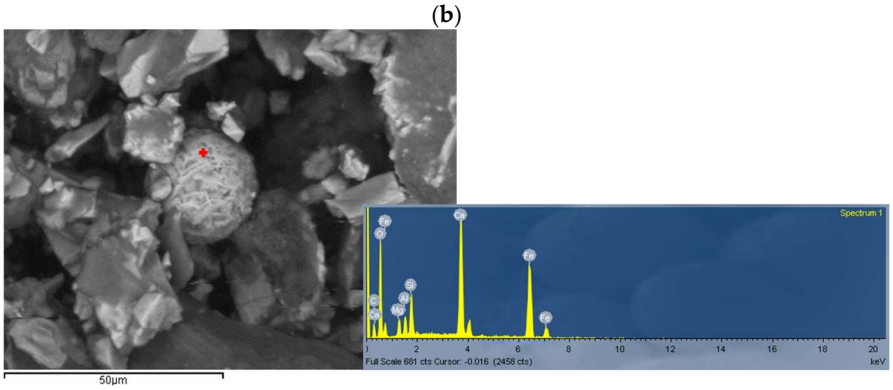

(**c**)

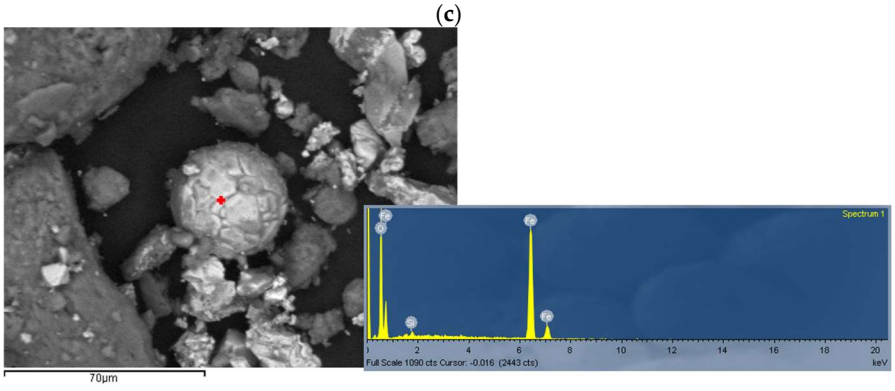

(**d**)

Figure 7. *Cont.*

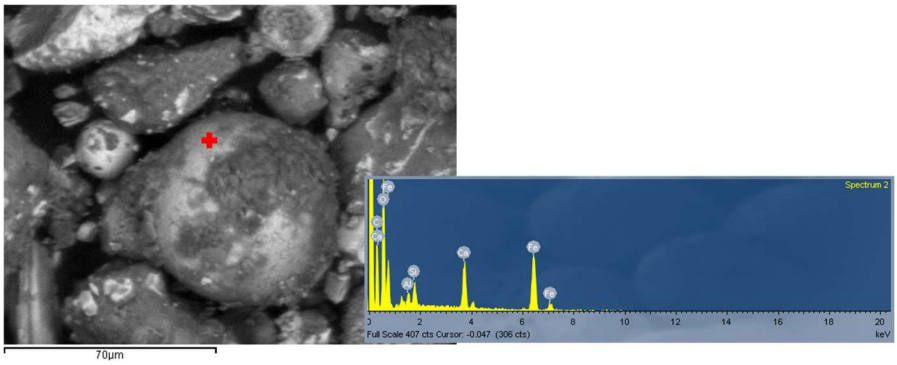

(**e**)

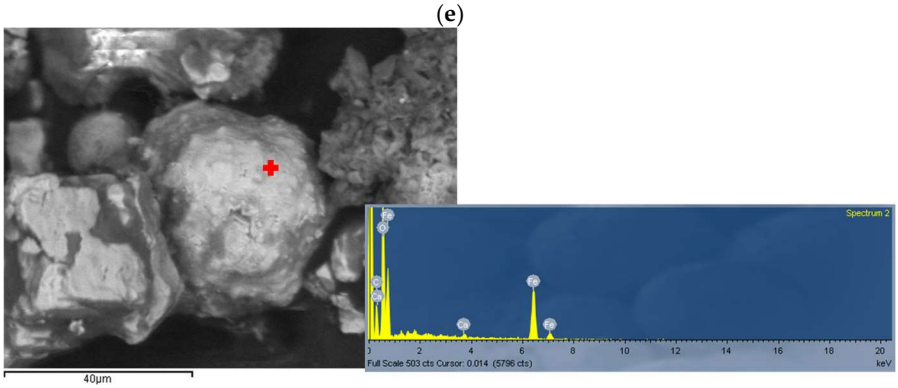

(**f**)

Figure 7. Magnetic particles in the form of spheres (**a**) with smooth surface structure; (**b**) as spongy type; (**c**) as thread type; (**d**) as blocky type; (**e**) with aluminosilicate aggregates; (**f**) with harsh surface as they were randomly observed with the scanning electron microscope. Red crosses correspond to the spots of analysis. The chemical composition of each particle is shown for each microphoto.

On the other hand, lithogenic magnetic particles (LMPs) in the form of octahedrons (pyramid-like) were also identified in the majority of samples B (50 cm depth). Their source seems to be mainly the ultramafic rocks in the NE and SW parts of the studied area. Figure 8a–c depicted some of them with usually very smooth surface structure (Figure 8a), a limited number of them are fragmented with their vertices being broken (Figure 8b), while multiple aggregated octahedrons are commonly found (Figure 8c). They are euhedral and their size ranges from 14 to 490 µm, similar to or slightly larger than that of the corresponding particles found in the shallower samples A, as the majority of them are between 50 and 100 µm. Particles with significantly larger diameters (>400 µm) were also found (Figure 7a).

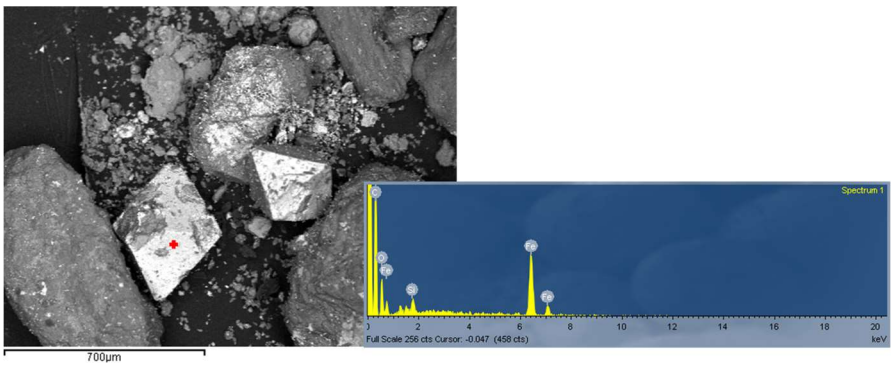

(**a**)

Figure 8. *Cont.*

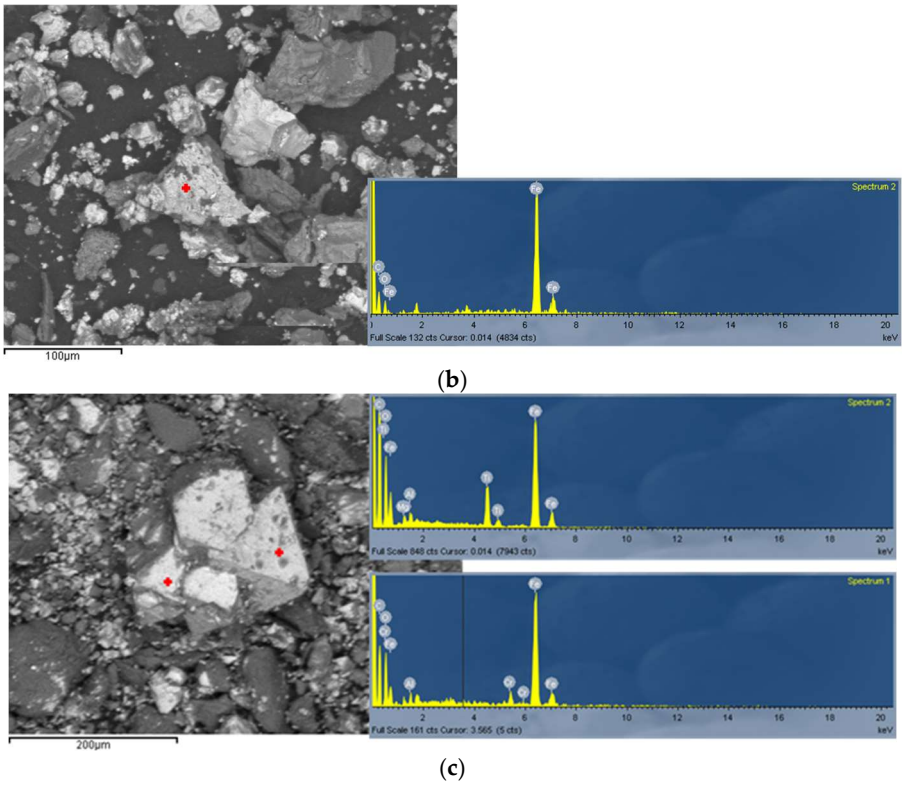

Figure 8. Magnetic particles from the studied samples in the form of octahedrons (**a**) with smooth surface structure; (**b**) fragmented with their vertices being broken; (**c**) as aggregates as they were randomly observed with the scanning electron microscope. Red crosses correspond to the spots of analysis. The chemical composition of each particle is shown for each microphoto.

Magnetite and titanomagnetite are omnipresent in soils and primary contributors of soil magnetism, deriving from lithogenic sources and pedogenic processes. As a member of the spinel group, magnetite can form solid solutions with other minerals of similar structure, including ulvospinel (Fe_2TiO_4) and magnesioferrite ($MgFe_2O_4$). Titanomagnetite may undergo oxy-exsolution during cooling, leading to the formation of magnetite and ilmenite [41].

In Figure 4, the highest positive and negative ΔX_{LF} values are found NW of Agios Dimitrios power plant and in the southern part of the study area, respectively. In both sampling profiles, AMPs and LMPs were identified. However, the same pattern applies to the majority of the studied samples, regardless of the main source that influences the values of ΔX_{LF} (fly ash dispersion or lithology of the area), indicating that neither of the two types of magnetic particle shows any preference of concentration in samples A or B.

According to the EDX analysis, Fe is the dominant element in the entire magnetic fraction with an average value of 71.5 wt.% for samples A and 65.9 wt.% for samples B. Al, Si, Mg and Ca are also found to accompany the majority of both octahedrons and spheres (3.30, 3.42, 3.32, 3.95 wt.%, respectively, for both sets of samples), consisting of components of the lithological formations of the study area or of the fly ash produced from the power plants. Cr seems to be present in both AMPs and LMPs with an average value of 7.63 wt.% and 9.92 wt.% for samples A and samples B, respectively. Ti was found in limited particles with an average value of 4.41 wt.% for samples A and 4.39 wt.% for samples B, while Mn (1.1 wt.%) and Zn (2.76 wt.%) were only detected in one magnetic sphere at the depth of 0–10 cm. Table 3 shows the average values for Fe, Cr and Ti separately for AMPs and LMPs.

Table 3. Average values (wt.%) for Fe, Cr and Ti of the total number of LMPs and AMPs.

	Fe	Cr	Ti
Total number of LMPs	70.17	9.40	4.6
Total number of AMPs	66.28	2.19	7.06

As expected, Fe is the most abundant element in the studied magnetic particles and it is present in higher amounts in the particles with a lithogenic source. Cr has an average value more than four times higher in the total amount of LMPs than in the AMPs, in contrast to Ti, which was found in almost double the AMPs than the LMPs. Numerous studies have shown that there is a strong link between heavy metals and magnetic particles, especially for anthropogenic, produced from industrial activity, vehicle and household emission sources [32,42–45]. Pollutants such as Ni, Cr and other heavy metals can be absorbed into magnetic particles and transported with them due to their large surface area [43]. Cr in the magnetic fraction comes from the surrounding ultrabasic rocks, as it appears in a higher percentage in particles of lithogenic origin, however, the contribution of fly ash particles is also important. A strong contribution of fly ash particles to the presence of Cr in the soils of the Kozani region has been indicated [21,22]. Mn, Zn and mainly Ti are components of magnetic spheres studied in fly ash samples produced by Agios Dimitrios and Kardia power plants [21,22,46]. In addition, Ti, as the most common substitute for Fe in lithogenic magnetite, has a justified presence in the identified magnetite crystals from the surrounding ultramafic rocks. Based on these findings, in combination with the results of the magnetic susceptibility measurements, the spread of the fly ash from Agios Dimitrios and Kardia power plants in the area of Sarigiol basin is highlighted. Magnetic particles with an anthropogenic source were identified at the depth of 50 cm, indicating the long-term footprints of these industrial activities. In addition, the presence of lithogenic magnetic particles and the negative ΔX_{LF} values (indication of lithogenic source) show the feeding path of the ophiolite material to the basin and its interaction with the pollutants.

3.3. Future Research

Magnetic susceptibility appears to be a very useful tool in the hands of the scientific community for measuring the magnetic properties of soils and determining the source of magnetic particles in them, especially in combination with the determination of their chemical composition through geochemical methods and their morphological characteristics. As such, a further systematic and detailed sampling directly north of the Ptolemaida region is needed to elucidate the broader effects of the dispersion of the fly ash derived from the industrial activity of the Kozani–Ptolemaida region and its impact on the environment and public health. More specifically, this may include:

1. Extension of the sampling mainly to the north of the Ptolemaida region but also to other areas in different directions which have not been covered yet and may possibly be affected by the fly ash dispersion. Different depths (even deeper than 50 cm) may provide useful information on the soil pollution level. In addition, a temporal monitoring program for seasonal sampling over the years or the seasons will enable the identification of fly ash accumulation trends, the seasonal effects on them but also the industrial activity of the broader region and the interaction with soil genesis and sedimentation.
2. Expansion of geochemical analysis to include a broader suite of trace elements which are often connected with industrial pollution and especially heavy metals with the magnetic susceptibility signals by using inductively coupled plasma mass spectrometry (ICP-MS) analysis.

3. Studying the interaction of fly ash dispersion and the fluctuations of the magnetic susceptibility with soil properties such as pH, organic matter content, vegetation and aquatic ecosystems for assessing the contamination effects on flora and fauna and possible ecological consequences such as disruption of biodiversity and soil fertility.
4. Air and water quality monitoring with modern filtering technologies for the identification of respiratory and other health issues linked to long-term exposure to pollutants.

These future plans aim to improve the understanding of the long-term effects of the fly ash pollution in the broader area of Kozani and Ptolemaida in northern Greece and offer some practical keys for sustainable environmental management and public health protection.

4. Conclusions

Sediment samples (38) were collected from 19 different locations in Sarigiol basin at depths of 0–10 (samples A) and 10–50 cm (samples B) in order to study their magnetic properties using the magnetic susceptibility method in vertical profiles. In addition, in a subset of samples, magnetic particles were studied to determine their chemical composition by EDX analysis, while their morphological characteristics were examined through scanning electron microscopy (SEM). The highest values for studied samples A and B have the same pattern and they were found in the NNE, E and S parts of the study area, in the vicinity of Agios Dimitrios power plant, the conveyor belt and SW of a significant ophiolite complex. These results agree with the spatial distribution of ΔX_{LF}, based on which the highest positive values of the ΔX_{LF} are presented west of Agios Dimitrios power plant (E part of the study area) and north of the conveyor belt (NE part of the study area). The negative values presented in the S and locally in the NE and W parts are attributed to the widespread occurrence of ultramafic rocks in the NE part of the basin and the scattered appearances of ophiolite complexes in the S and W parts. Most of the study area shows positive values indicating the influence of the anthropogenic activities and especially of the fly ash dispersion and deposition to the depth of 50 cm. The highest values of X_{FD} % for the samples are limited in the SE and locally in the S and W parts of the basin for samples A and B, respectively, indicating that SP grains probably from pedogenic processes seem to be present in significant amounts. Correlation between X_{LF} and X_{FD} values for the studied samples is very weak, while the majority of the samples have X_{FD} % values between 2 and 10%, indicating an admixture of SP and coarser non-SP grains or even smaller SP grains. The contribution of the fly ash particles plays a primary role as the wider area of Ptolemaida–Kozani is highly industrialized.

Morphological observation of random AMPs identified them even deeper at the depth of 10–50 cm, with most of them having a complex surface structure with crystalline patterns, corresponding to the combustion of fossil fuels at high temperatures. The majority of the magnetic spheres have a size range between 10 and 50 μm for the total profile, in contrast to the majority of the identified LMPs, the size of which is 50–100 μm with even bigger particles with a diameter larger than 400 μm. In addition, their surface is very smooth and a limited number of them have irregular shapes. The two types of magnetic particles do not appear exclusively in any of the two sets of samples A and B, indicating the effect of fly ash dispersion throughout the sampling profiles of the study area. Fe is the dominant element of the magnetic particles in samples A and B. Its average value decreases with depth, while its value is higher in the LMPs than in AMPs. Cr was detected in a higher percentage in the LMPs than in the AMPs, which is combined with the increased average value with depth indicating that its source is mainly the ultramafic rocks. Mn and Zn were found only in one magnetic sphere at the depth of 0–10 cm, while Ti had a slightly higher percentage in both LMPs and AMPs, but a decreasing average value with depth, indicating the contribution

of the fly ash particles. Based on the total findings, it is made clear that by examining the magnetic properties of the sediments in Sarigiol basin, the present study provides a clear indication of how power plant activity and especially fly ash transportation and deposition affect the surrounding environment. Magnetic susceptibility is highlighted as an effective tool for monitoring environmental pollution and, consequently, these findings may be used as important keys for assessing long-term environmental consequences.

Author Contributions: Conceptualization, C.C. and N.K.; methodology, C.C., E.A., D.V., A.D., L.P. and N.K.; investigation, C.C.; data curation, C.C. and E.A.; writing—original draft preparation, C.C.; writing—review and editing, C.C., E.A. and N.K.; visualization, C.C. and E.A.; supervision, N.K. All authors have read and agreed to the published version of the manuscript.

Funding: This study is part of the research of the first author, C. Chrysakopoulou, which is financed by the Special Account for Research Funds AUTH, Grant No. 373423.

Data Availability Statement: Data are contained within the article.

Conflicts of Interest: The authors declare no conflicts of interest.

Abbreviations

The following abbreviations are used in this manuscript:

PM_{10}	Particulate matter below 10 μm
MS	Magnetic susceptibility
χ	Mass-specific magnetic susceptibility
X_{FD}	Frequency dependent susceptibility
EDX	Energy dispersive X-ray analysis
SEM	Scanning electron microscopy
X_{LF}	Low-field mass-specific magnetic susceptibility
ΔX_{LF}	Difference of the low-field mass-specific magnetic susceptibility
SP	Superparamagnetic
MD	Multidomain
AMPs	Anthropogenic magnetic particles
LMPs	Lithogenic magnetic particles
ICP-MS	Inductively coupled plasma mass spectrometry

References

1. Landrigan, P.J.; Fuller, R.; Acosta, N.J.R.; Adeyi, O.; Arnold, R.; Basu, N.; Baldé, A.B.; Bertollini, R.; Bose-O'Reilly, S.; Boufford, J.I.; et al. The Lancet Commission on pollution and health. *Lancet* **2018**, *391*, 462–512. [CrossRef]
2. Adami, G.; Pontalti, M.; Cattani, G.; Rossini, M.; Viapiana, O.; Orsolini, G.; Benini, C.; Bertoldo, E.; Fracassi, E.; Gatti, D.; et al. Association between long-term exposure to air pollution and immune-mediated diseases: A population-based cohort study. *RMD Open* **2022**, *8*, e002055. [CrossRef] [PubMed]
3. Menshov, O.; Vyzhva, S.; Horoshkova, L.; Tonkha, O.; Ivanik, O.; Pereira, P.; Dindaroglu, T.; Pastushenko, T.; Eiben, H. Distribution of soil magnetic susceptibility as a pollution indicator in the urban and tourist city of Lviv, Ukraine. *Environ. Earth Sci.* **2023**, *82*, 486. [CrossRef]
4. Magiera, T.; Gołuchowska, B.; Jabłonska, M. Technogenic Magnetic particles in alkaline dusts from power and cement plants. *Water Air Soil Pollut.* **2013**, *224*, 1389. [CrossRef] [PubMed]
5. Aidona, E.; Grison, H.; Petrovsky, E.; Kazakis, N.; Papadopoulou, L.; Voudouris, K. Magnetic characteristics and trace elements concentration in soils from Anthemountas River basin (North Greece): Discrimination of different sources of magnetic enhancement. *Earth Sci.* **2016**, *75*, 1375. [CrossRef]
6. Bucko, M.S.; Magiera, T.; Johansond, B.; Petrovskýe, E.; Pesonena, L.J. Identification of magnetic particulates in road dust accumulated on roadside snow using magnetic, geochemical and micro-morphological analyses. *Environ. Pollut.* **2011**, *159*, 1266–1276. [CrossRef] [PubMed]
7. Grimley, D.A.; Lynn, A.S.; Brown, C.W.; Blair, N.E. Magnetic Fly Ash as a Chronological Marker in Post-Settlement Alluvial and Lacustrine Sediment: Examples from North Carolina and Illinois. *Minerals* **2021**, *11*, 476. [CrossRef]

8. Kapicka, A.; Jordanova, N.; Petrovsky, E.; Ustjak, S. Effect of different soil conditions on magnetic parameters of power-plant fly ashes. *J. Appl. Geophys.* **2001**, *48*, 93–102. [CrossRef]
9. Vasiliev, A.; Gorokhova, S.; Razinsky, M. Technogenic Magnetic Particles in Soils and Ecological–Geochemical Assessment of the Soil Cover of an Industrial City in the Ural, Russia. *Geosciences* **2020**, *10*, 443. [CrossRef]
10. Wawer, M. Identification of Technogenic Magnetic Particles and Forms of Occurrence of Potentially Toxic Elements Present in Fly Ashes and Soil. *Minerals* **2020**, *10*, 1066. [CrossRef]
11. Wilczyńska-Michalik, W.; Michalik, J.M.; Kapusta, C.; Michalik, M. Airborne Magnetic Technoparticles in Soils as a Record of Anthropocene. *Atmosphere* **2020**, *11*, 44. [CrossRef]
12. Ji, M.; Ling, H.; Liu, L.; Yang, Y.; Chen, M.; Yang, D.; Liu, H. Comparison of magnetic susceptibility probes relevantly used in soil contamination applications. *Environ. Monit. Assess.* **2023**, *195*, 677. [CrossRef]
13. ZawadzkiJ, J.; Fabijańczyk, P.; Magiera, T.; Marzena, R. Geostatistical Microscale Study of Magnetic Susceptibility in Soil Profile and Magnetic Indicators of Potential Soil Pollution. *Water Air Soil Pollut.* **2015**, *226*, 142. [CrossRef]
14. Dearing, J.A. *Environmental Magnetic Susceptibility: Using the Barrington MS2 System*, 1st ed.; Chi Pub: Kenilworth, UK, 1994.
15. Thompson, R.; Oldfield, F. *Environmental Magnetism*, 1st ed.; Allen & Unwin Ltd.: London, UK, 1986. [CrossRef]
16. Magiera, T.; Strzyszcz, Z.; Kapicka, A.; Petrovsky, E. Discrimination of lithogenic and anthropogenic influences on topsoil magnetic susceptibility in Central Europe. *Geoderma* **2006**, *130*, 299–311. [CrossRef]
17. Fialova, H.; Maier, G.; Petrovsky, E.; Kapicka, A.; Boyko, T.; Scholger, R. Magnetic properties of soils from sites with different geological and environmental settings. *J. Appl. Geophys.* **2006**, *59*, 273–283. [CrossRef]
18. Sarris, A.; Kokkinou, E.; Aidona, E.; Kallithrakas-Kontos, N.; Koulouridakis, P.; Kakoulaki, G.; Droulia, K.; Damianovits, O. Environmental study for pollution in the area of Megalopolis Power Plant (Peloponnesus, Greece). *Environ. Geol.* **2009**, *58*, 1769–1783. [CrossRef]
19. Bourliva, A.; Papadopoulou, L.; Aidona, E.; Giouri, K. Magnetic signature, geochemistry, and oral bioaccessibility of "technogenic" metals in contaminated industrial soils from Sindos Industrial Area, Northern Greece. *Environ. Sci. Pollut. Res.* **2017**, *24*, 17041–17055. [CrossRef] [PubMed]
20. Menegaki, S.; Kelepertzis, E.; Kypritidou, Z.; Lampropoulou, A.; Chrastný, V.; Aidona, E.; Bourliva, A.; Komárek, M. Characterization of the inhalable fraction (<10 μm) of soil from highly urbanized and industrial environments: Magnetic measurements, bioaccessibility, Pb isotopes and health risk assessment. *Environ. Geochem. Health* **2024**, *46*, 230. [CrossRef]
21. Kazakis, N.; Kantiranis, N.; Kalaitzidou, K.; Kaprara, E.; Mitrakas, M.; Frei, R.; Vargemezis, G.; Tsourlos, P.; Zouboulis, A.; Filippidis, A. Origin of hexavalent chromium in groundwater: The example of Sarigkiol Basin, Northern Greece. *Sci. Total Environ.* **2017**, *593*, 552–566. [CrossRef] [PubMed]
22. Kazakis, N.; Kantiranis, N.; Kalaitzidou, K.; Kaprara, E.; Mitrakas, M.; Frei, R.; Vargemezis, G.; Vogiantzis, D.; Zouboulis, A.; Filippidis, A. Environmentally available hexavalent chromium in soils and sediments impacted by dispersed fly ash in Sarigkiol basin (Northern Greece). *Environ. Pollut.* **2018**, *235*, 632–641. [CrossRef]
23. Kolovos, N.; Georgakopoulos, A.; Filippidis, A.; Kavouridis, C. Environmental effects of lignite and intermediate steriles coexcavation in the southern lignite field mine of Ptolemais, northern Greece. *Energy Sources* **2002**, *24*, 561–573. [CrossRef]
24. Chrysakopoulou, C.; Vogiatzis, D.; Drakoulis, A.; Papadopoulou, L.; Kantiranis, N. Heavy Metal Load in Airborne Magnetic Particles from Anthropogenic Activities in a Contaminated Area in Northern Greece and Their Environmental Impact. *Environ. Sci. Proc.* **2023**, *26*, 212. [CrossRef]
25. Chrysakopoulou, C.; Vogiatzis, D.; Drakoulis, A.; Papadopoulou, L.; Kantiranis, N. Morphological characteristics of magnetic particles and their environmental impact: The case of Sarigiol basin (Greece). *E3S Web Conf.* **2023**, *436*, 08007. [CrossRef]
26. CityPolulation.de. Available online: https://www.citypopulation.de/en/greece/cities/?cityid=19728 (accessed on 14 October 2024).
27. Petrotou, A.; Skordas, K.; Papastergios, G.; Filippidis, A. Concetrations and bioavailability of potentially toxic elements in soils of an industialised area of northwestern Greece. *Fresenius Environ. Bull.* **2010**, *19*, 2769–2776.
28. Wang, L.; Liu, D.; LÜ, H. Magnetic susceptibility properties of polluted soils. *Chin. Sci. Bull.* **2000**, *45*, 1723–1726. [CrossRef]
29. Roberts, A.P. Magnetic mineral diagenesis. *Earth-Sci. Rev.* **2015**, *151*, 1–47. [CrossRef]
30. Wojas, A. The magnetic susceptibility of soils in Krakow, southern Poland. *Acta Geophys.* **2017**, *65*, 453–463. [CrossRef]
31. Kanu, M.O.; Meludu, O.C.; Oniku, S.A. Comparative study of top soil magnetic susceptibility variation based on some human activities. *Geofis. Int.* **2014**, *53*, 411–423. [CrossRef]
32. Hanesch, M.; Scholger, R. Mapping of heavy metal loadings in soils by means of magnetic susceptibility measurements. *Environ. Geol.* **2002**, *42*, 857–870. [CrossRef]
33. Maher, B. Characterisation of soils by mineral magnetic measurements. *Phys. Earth Planet. Inter.* **1986**, *42*, 76–92. [CrossRef]
34. Hanesch, M.; Scholger, R. The influence of soil type on the magnetic susceptibility measured throughout soil profiles. *Geophys. J. Int.* **2005**, *161*, 50–56. [CrossRef]
35. Lu, S.G.; Bai, S.Q. Study on the correlation of magnetic properties and heavy metals content in urban soils of Hangzhou City, China. *J. Appl. Geophys.* **2006**, *60*, 1–12. [CrossRef]

36. Dearing, J.A.; Dann, R.J.L.; Hay, K.; Lees, J.A.; Loveland, P.J.; Maher, B.A.; O'Grady, K. Frequency-dependent susceptibility measurements of environmental materials. *Geophys. J. Int.* **1996**, *124*, 228–240. [CrossRef]
37. Hamdan, A.M.; Syafrina, S.L.; Nazlaa, C.T.; Jaswitaa, D.; Maulidaa, Z.; Munandara, A.; Hamdib, H.; Ardiansyaha, R.; Khairuzzamana, H. Magnetic susceptibilites of suspended sediment and microplastic abundance in a tropical volcanic estuary. *Reg. Stud. Mar. Sci.* **2023**, *61*, 102927. [CrossRef]
38. Han, Y.; Liu, X.; Zhao, G.; Lü, B.; Chen, Q. Magnetic monitoring of topsoil and street dust in Xinyang (China) and their environmental implications. *Environ. Monit. Assess.* **2021**, *193*, 602. [CrossRef] [PubMed]
39. Adachi, K.; Tainosho, Y. Characterization of heavy metal particles embedded in tire dust. *Environ. Int.* **2004**, *30*, 1009–1017. [CrossRef]
40. Ault, A.P.; Peters, T.M.; Sawvel, E.J.; Casuccio, G.S.; Willis, R.D.; Norris, G.A.; Grassian, V.H. Single-particle SEM-EDX analysis of iron-containing coarse particulate matter in an urban environment: Sources and distribution of iron within Cleveland, Ohio. *Environ. Sci. Technol.* **2012**, *46*, 4331–4339. [CrossRef] [PubMed]
41. Nesse, W.D. *Introduction to Mineralogy*, 1st ed.; Oxford University Press: New York, NY, USA, 1999; p. 361, ISBN 9780195106916.
42. Bourliva, A.; Papadopoulou, L.; Aidona, E. Study of road dust magnetic phases as the main Carrier of potentially harmful trace elements. *Sci. Total Environ.* **2016**, *553*, 380–391. [CrossRef] [PubMed]
43. Bourliva, A.; Aidona, E.; Papadopoulou, L.; Ferreira da Silva, E.; Patinha, C.; Sarafidis, C.; Kantiranis, N. An integrated approach combining magnetic, geochemical and particle-based techniques to assess metal (loid) loadings in urban venues frequented by children. *Sci. Total Environ.* **2022**, *822*, 153600. [CrossRef] [PubMed]
44. Tan, F.M.; Yang, H.Y.; He, J.; Wang, K.; Zhang, N.M. Study on the relationship between soil magnetic susceptibility and heavy metal content around the mining area—Taking Cangyuan and Gejiu lead zinc mines as an example. *Chin. J. Soil Sci.* **2021**, *52*, 192–197. [CrossRef]
45. Kim, W.; Doh, S.J.; Yu, Y. Anthropogenic contribution of magnetic particulates in urban roadside dust. *Atmos. Environ.* **2009**, *43*, 3137–3144. [CrossRef]
46. Iordanidis, A.; Buckman, J.; Triantafyllou, A.G.; Asvetsa, A. Fly ash–airborne particles from Ptolemais–Kozani area, northern Greece, as determined by ESEM-EDX. *Int. J. Coal Geol.* **2008**, *73*, 67–69. [CrossRef]

Disclaimer/Publisher's Note: The statements, opinions and data contained in all publications are solely those of the individual author(s) and contributor(s) and not of MDPI and/or the editor(s). MDPI and/or the editor(s) disclaim responsibility for any injury to people or property resulting from any ideas, methods, instructions or products referred to in the content.